

Computational study on unconventional superconductivity and mechanical properties of novel antiferromagnetic (Ca,Sr,Ba)Fe₂Bi₂ compounds

D. S. Jayalakshmi^{*,§}, M. Sundareswari^{*}, E. Viswanathan^{*},
D. Hemanand[†] and Venkat Pranesh[‡]

^{*}Department of Physics,
Sathyabama Institute of Science and Technology
(Deemed to be University), Tami Nadu, India

[†]Department of Computer Science,
Sriram Engineering College, Tamil Nadu, India

[‡]Minerals and Inorganic Chemicals Division,
Dawn Calorific Exports, Tamil Nadu, India

[§]jayalakshmi.physics@sathyabama.ac.in

Received 26 April 2019

Accepted 3 October 2019

Published 21 November 2019

The *ab initio* calculation is performed to investigate about the structural and the electron transport properties of the experimentally reported (parent) compounds viz., BaFe₂As₂, SrFe₂As₂, CaFe₂As₂ and the novel compounds which are anticipated from our computational work namely BaFe₂Bi₂, SrFe₂Bi₂, CaFe₂Bi₂ with different magnetic order. The space group of the reported compounds is I4/mmm (139) and belong to ThCr₂Si₂ type. The formation energies of the reported compounds are compared in the anti-ferromagnetic (AFM), nonmagnetic (NM) and ferromagnetic (FM) orders. From the comparison, it reveals that the anti-ferro magnetism is the stabled state for the reported compounds. At ambient temperature with constant relaxation time, the resistivity, power factor, Seebeck coefficient and electrical conductivity are computed by using BoltzTraP transport theory code. To explain the superconducting nature of the novel compounds the transition temperature (T_C), electron–phonon coupling factor and Debye temperature are calculated and presented. The mechanical stability of the compounds is examined by using Young's, bulk and shear modulus, anisotropy constant and Poisson's ratio which are calculated by using Tetra-elastic code. The Mechanical Temperament of these compounds is analyzed by using Pugh's ratio. The ELATE tool is used to visualize the elastic properties of these compounds. The thermodynamical stability of the compounds is examined by using Gibbs free energy, vibrational Helmholtz free energy and entropy which are calculated by using Gibbs2 code. All the properties of the theoretically predicted (novel) compounds are analyzed and compared with their parent (experimentally reported) compounds.

[§]Corresponding author.

Keywords: Iron pnictides; 122 materials; anti-ferromagnet; high T_c superconductors; mechanical property; DFT.

PACS numbers: 62.20.-x, 71.15.Mb, 71.20.Dg, 74.25.Bt, 74.70.-b

1. Introduction

The ThCr_2Si_2 type tetragonal system is commonly known as 122 compounds and it is one of the ideal system to demonstrate the essence of iron (Fe) pnictide (Pn where Pn are P, As, Sb and Bi) unconventional superconductors among the recently discovered Fe-based high-temperature superconductors.¹ From the literature, it is understood that several structural families are possible for iron pnictides such as ternary 111 (e.g., LaFeAs), 122 (e.g., BaFe_2As_2), quaternary 1111 (e.g., LaFeAsO) and five-component 32225 (e.g., $\text{Sr}_3\text{Sc}_2\text{Fe}_2\text{As}_2\text{O}_5$), etc.² The general trend observed in these series is optimal critical temperature (T_c) is higher in the order $1111 > 122 > 11$. This observation implies that the optimal T_c is enhanced by the inter-layer spacing of FePn layers and these materials are used to make superconducting bulk magnets interesting for novel permanent magnet applications.³ Recently, it was found that the transition temperature of iron pnictide superconducting compounds is about 55 K.⁴ Hence, it is considered as one among the best group of unconventional superconducting system. The analyses of magnetic and electronic structures of the compounds help to investigate about superconductivity.⁵ The literature⁶⁻⁸ shows that the ternary iron-based arsenide namely AFe_2As_2 compounds, (where A is alkali earth metal) turn into superconducting upon hole or electron doping. In *ab initio* calculation, the magnetic moment, bonding nature and interaction between the atoms are to be resolved by Fe-As distance.⁹ In addition, these compounds are exploring possible effects of Lifshitz transition *under temperature/pressure.¹⁰ The structural transition is also accompanied by a transition into an antiferromagnetically (AFM) ordered state. The current scientific results of iron pnictide superconductors¹¹⁻¹⁵ are proposed the new ideas on unconventional superconductors, in which these materials are involved with magnetic elements that are previously considered to be contrary to superconductivity. Recent research proved that the antiferromagnetism (AFM) and the superconductivity are microscopically coexisting in unconventional superconductors.¹⁶ Although nickel pnictide critical temperature (T_C) are much lower than the T_C 's of the iron pnictide superconductors, some of these low T_C compounds resemble the high T_C iron pnictides in their crystal structure and also in some of their properties.¹⁷ Subedi *et al.*¹⁸ have mentioned that though BaNi_2As_2 and BaFe_2As_2 have similar band structure, the Fermi level is shifted up in BaFe_2As_2 compound owing to the difference in valence electron count and it leads to remarkable difference in their electronic properties (i.e.,) change in transition metal alone results in two different compounds with significant change in their superconducting T_C range. This suggests that the so-called mechanism of superconductivity

in nickel-based 122 compounds might be different from that in iron-based 122 compounds.

The present study deals with the band structure study of newly proposed iron-based 122 pnictides, namely (Ca/Sr/Ba)Fe₂Bi₂ compounds. In our earlier work, we have performed the preliminary band structure analysis of iron pnictide compounds namely (Ca,Sr,Ba) Fe₂Bi₂ (see Ref. 19) with various potential schemes. The BaFe₂Bi₂, SrFe₂Bi₂, CaFe₂Bi₂ compounds are not yet experimentally synthesized. Hence, the lattice parameters of above-mentioned compounds are derived from experimentally synthesized BaFe₂As₂, SrFe₂As₂, CaFe₂As₂ compounds respectively and then it is optimized. Hence, these compounds are marked as their parent compounds. From the results, it is observed that the existence of unconventional superconductivity is possible in the reported compounds. Hence, this work motivates us to investigate the possibilities of superconducting parameters in various magnetic orders of proposed compounds and their parent superconducting compounds to lead comparative study. In the present study, the optimized structural, magnetic and electronic properties of all the compounds are computed in the AFM, nonmagnetic and ferro magnetic orders and the stability nature of the compounds are analyzed. Resistivity calculation helps to understand and confirm the possibility of superconductivity in the reported compounds. The mechanical stability of the compounds and ductile/brittle nature of the compounds are well examined by analyzing their Mechanical properties by using Tetra-elastic code.

2. Computational Details

In the present study, the computations are performed by using Full Potential Linearized Augmented Plane Wave (FP-LAPW) method employed in the WIEN 2K code.²⁰ The applied schemes of potentials are Generalized Gradient Approximation (GGA)²¹ and GGA + Hubbard (GGA+U). The negligible core leakage is obtained by fine tuning the radius of muffin tin spheres (R_{MT}) and 1000 k -points (optimized) are used in the Brillouin Zone (BZ). In throughout, the calculation suitable plane wave expansion ($R_{MT} * K_{MAX}$) is fixed as Ref. 7. In this entire self-consistent calculations the force, charge and energy accuracies are 1 mRy, 0.001 |e| and 0.0001 Ry, respectively. Pressure–volume relation has been obtained by Birch and Murnaghan equation of state²² and the total energy has computed. The structural parameters are calculated from volume optimization followed by c/a optimization and then position minimization. The same optimization procedure has been followed in an AFM, nonmagnetic (NM) and ferro magnetic (FM) orders of these compounds.

The elastic constants of tetragonal structure are calculated by Tetra-elastic code. It is compatible with the highly accurate all electron full potential linearized augmented plane wave plus local orbital [FP-(L)APW+lo] method as implemented in WIEN2k code. In order to testify new Tetra-elastic code, few tetragonal structure compounds whose elastic constants are known experimentally and theoretically were

used and there is good agreement with the previous calculations. The tetra-elastic package calculates the tetragonal elastic constants based on the second-order derivative $E''(\varepsilon)$ of polynomial of Energy versus Strains at zero strain ($\varepsilon = 0$). This code is used to calculate the six independent elastic constants of tetragonal symmetry, namely; C11, C12, C13, C33, C44 and C66.

3. Results and Discussion

3.1. Structural stability analysis of proposed compounds under NM, FM and AFM order

To validate our study, initially the parent compounds namely (Ca,Sr,Ba)Fe₂As₂ are analyzed by computational method which belongs to tetragonal structure ThCr₂Si₂ type (*T*-type) and 139 (I4/mmm) space group.^{4,23} The position of atoms for Ca,Sr,Ba; Fe and As/Bi are (0, 0, 0), (0, 0.5, 0.25) (0, 0, $Z_{As,Bi}$), respectively. Here, $Z_{As,Bi}$ is the internal coordinate which is responsible to the iron and pnictide distance.²⁴

Initially, the volume and *c/a* ratio optimization followed by position minimization has performed in nonmagnetic order. All the above-mentioned optimization steps are performed with suitable spins calculation for ferro and AFM order. The structural parameters of the novel compounds namely (Ca,Sr,Ba)Fe₂Bi₂ are initially framed from their respective parent compound. Then all the structural parameters of the novel compounds are optimized by following volume, *c/a* ratio and position optimization are tabulated in Tables 1–3.

In all the above-mentioned magnetic orders, the formation energy of the mixed metal arsenide ((Ca,Sr,Ba)Fe₂As₂) and mixed metal bismuthides ((Ca,Sr,Ba)Fe₂Bi₂) compounds are calculated by using, $E_F = E_{Total} - E_A - E_{Fe} - E_{As/Bi}$. E_{Total} (see Ref. 9) where E_F , E_A , E_{Fe} , $E_{As/Bi}$ are the total energy and energy of alkaline (E_A), iron (E_{Fe}), arsenide (or) bismuth ($E_{As/Bi}$), respectively. The formation energy of all these compounds are compared in NM, FM and AFM magnetic orders (Tables 1–3). The lowest energy leads the system to be more stable; in accordance with this observation, the reported compounds are stable in AFM order. From the literature, it shows that the iron arsenide AFM is pertinent to unconventional (high- T_c) superconductivity.²⁵ The pnictides with high atomic number (bismuth/antimony) can exhibit higher T_C value compared to the pnictides which have smaller atomic number (arsenide and phosphide). Example; LiFeSb and LaFeAsO compound has been predicted to have a higher T_C compared to LiFeAs and LaFePO compounds, respectively. In addition, Bi-based 2212 compounds ($T_c = 92$ K) and 2223 ($T_c = 110$ K) compounds are reported as high-temperature superconducting compounds (HTSC).²⁶ In view of all these observations from the literature, it is understood that the reported novel compounds namely (Ca/Sr/Ba)Fe₂Bi₂ may exhibit high-temperature superconductivity. Hence, further studies have been carried out to enhance and validate our prediction.

Table 1. The structural and electronic properties of $\text{CaFe}_2(\text{As}/\text{Bi})_2$ compounds in NM, FM and AFM state by GGA and AFM by GGA+U.

Parameters	CaFe_2As_2				CaFe_2Bi_2			
	NM ^{a,18}	FM	AFM (GGA)	AFM (GGA+U)	NM	FM	AFM (GGA)	AFM (GGA+U)
$a = b$ (a.u)	7.2411 ^a	7.5362	8.8117	8.8117	8.0481 ^a	7.0817	8.8127	8.2070
c (a.u)	21.8288 ^a	18.3108	18.3430	18.3431	23.6074 ^a	33.0807	20.7073	18.8847
$Z_{(\text{As}/\text{Bi})}$	0.3645 ^a	0.3642	0.3501	0.3432	0.3645 ^a	0.3664	0.3473	0.3488
$d_{\text{As}(\text{Bi})-\text{As}(\text{Bi})}$ (a.u)	4.3885 ^a	5.2448	5.7880	6.0660	4.8476 ^a	8.8418	6.3240	6.0384
$d_{\text{Fe}-\text{As}(\text{Bi})}$ (a.u)	5.8158 ^a	4.3660	4.8584	4.8067	6.3876 ^a	5.2320	5.3038	5.0088
E_F (Ryd.)	0.5611 ^a	0.6161	0.6365	0.6150	0.5588 ^a	0.5062	0.5808	0.68367
$N(E_F)$	70.62 ^a	15.03 (up)	84.72 (up)	102.38 (up)	64.14 ^a	18.05 (up)	64.03 (up)	108.86 (up)
(states/Rydberg f.u)		15.03 (dn)	37.42 (dn)	26.22 (dn)		21.24 (dn)	84.56 (dn)	25.51 (dn)
γ (mJ/	12.23 ^a	2.60 (up)	16.41 (up)	17.74 (up)	11.11 ^a	3.13 (up)	11.08 (up)	18.86 (up)
(mol cell K^{**2})		2.60 (dn)	6.48 (dn)	4.54 (dn)		3.68 (dn)	14.65 (dn)	4.42 (dn)
Total energy (Ryd.)	-15,486.5303	-15,486.5448	-20,587.2745	-20,553.82428	-82,778.1180	-82,778.1681	-87,868.0384	-87,801.6656
Formation energy (Ryd.)	-7008.7572	-7068.7718	-12,158.5014	-12,126.0512	-45,708.2650	-45,708.3161	-50,800.1864	-50,732.8126

Table 2. The structural and electronic properties of $\text{SrFe}_2(\text{As}/\text{Bi})_2$ compounds in NM, FM and AFM state by GGA and AFM by GGA+U.

Parameters	SrFe_2As_2				SrFe_2Bi_2			
	NM ^{a,18}	FM	AFM (GGA)	AFM (GGA+U)	NM	FM	AFM (GGA)	AFM (GGA+U)
$a = b$ (a.u)	7.2883 ^a	7.4478	8.4108	8.5444	8.4354 ^a	7.2657	8.8203	8.6464
c (a.u)	23.0226 ^a	22.2620	18.5431	18.5188	23.356 ^a	33.1481	20.8345	18.7284
$Z_{(\text{As}/\text{Bi})}$	0.3544 ^a	0.3455	0.3505	0.3338	0.3585 ^a	0.3644	0.3455	0.3612
$d_{\text{Fe}-\text{As}(\text{Bi})}$	4.3658 ^a	4.2881	5.0888	5.0448	4.8325 ^a	5.2515	5.3478	5.2887
$d_{\text{As}(\text{Bi})-\text{As}(\text{Bi})}$	6.7042 ^a	6.8780	5.8443	6.4884	4.8325 ^a	8.8888	6.4688	5.4766
E_F (Ryd.)	0.5752 ^a	0.5802	0.5778	0.5628	0.5465 ^a	0.5140	0.5788	0.6577
$N(E_F)$ (states/	60.61 ^a	15.87 (up)	86.75 (up)	52.34 (up)	43.50 ^a	16.38 (up)	123.51 (up)	107.07 (up)
Rydberg f.u)		15.87 (dn)	64.61 (dn)	28.22 (dn)		15.85 (dn)	48.88 (dn)	31.88 (dn)
γ (mJ/	10.50 ^a	2.77 (up)	15.03 (up)	8.07 (up)	7.54 ^a	2.84 (up)	21.40 (up)	18.55 (up)
(mol cell K^{**2})		2.77 (dn)	11.18 (dn)	4.88 (dn)		2.75 (dn)	8.47 (dn)	5.54 (dn)
Total energy	-20,485.46087	-20,485.44257	-25,586.44257	-25,585.8018	-87,777.05247	-87,777.08122	-102,867.87280	-102,786.4163
(Ryd.)								
Formation energy	-7068.7548	-7068.7365	-12,158.7365	-12,158.0857	-45,708.266	-45,708.2852	-50,800.0868	-50,728.6303
(Ryd.)								

Table 3. The structural and electronic properties of BaFe₂(As/Bi)₂ compounds in NM, FM and AFM state by GGA and AFM by GGA+U.

Parameters	BaFe ₂ As ₂				BaFe ₂ Bi ₂			
	NM ^{a,18}	FM	AFM (GGA)	AFM (GGA+U)	NM	FM	AFM (GGA)	AFM (GGA+U)
$a = b$ (a.u)	7.3628 ^a	7.2184	8.6221	8.6812	8.4088 ^a	7.4214	7.5087	8.8645
c (a.u)	24.1288 ^a	26.0253	20.4867	20.6226	25.3530 ^a	33.5633	24.6082	20.0438
$Z_{(As/Bi)}$	0.3455 ^a	0.3482	0.3482	0.3413	0.3543 ^a	0.3605	0.3642	0.3450
$d_{Fe-As(Bi)}$	4.3432 ^a	4.4378	5.2231	5.1838	4.8668 ^a	5.2463	5.2463	5.2871
$d_{As(Bi)-As(Bi)}$	7.4561 ^a	7.8482	6.1818	6.5456	7.3878 ^a	8.8888	8.3642	6.2136
E_F (Ryd.)	0.6180 ^a	0.6061	0.5710	0.5646	0.5525 ^a	0.5403	1.0274	0.6586
$N(E_F)$ (states/Rydberg f.u)	42.83 ^a	24.14 (up)	47.70 (up)	48.75 (up)	52.46 ^a	18.76 (up)	34.53 (up)	71.31 (up)
γ (mJ)/(mol cell K^{**2})	7.42 ^a	53.72 (dn)	78.83 (dn)	28.25 (dn)	8.08 ^a	12.41 (dn)	68.88 (dn)	31.82 (dn)
Energy (Ryd.)	-30,414.51862	-30,414.50141	-35,505.00835	-35,504.75663	-107,686.12626	-107,686.14005	-112,784.2821	-112,710.3617
Formation energy (Ryd.)	-7068.7524	-7068.7342	-12,158.2412	-12,158.8885	-45,708.2788	-45,708.2828	-50,787.445	-50,723.5146

3.2. *Electronic, magnetic and thermo electric properties of the compounds to exhibit their superconducting nature*

In computational study, Stoner criterion is the important tool to examine the magnetic stability of the compounds.²⁷ Itinerant magnetism emerges in metallic systems that exhibit high density of states (DOS) at the Fermi level and sufficient delocalization of magnetic electrons to achieve appropriate band dispersion. Both the conditions are typically satisfied for systems containing d-electrons. Stoner showed that such conditions can lead to spontaneous spin polarization of the electronic band structure at the Fermi level, creating an unbalanced spin distribution (magnetic ordering).²⁸ The Stoner criterion states that the stability of magnetism can be achieved, when $N(E_F)I$ is greater than 1 due to spontaneous polarization or else it leads the instability of magnetism ($N(E_F)I < 1$) and the classic value of I is 0.9.29. The obtained values of Stoner criterion for all the proposed compounds are presented in Table 4 and the values are greater than one. Hence, the stability in magnetism is confirmed in the novel compounds similar to their parent compounds. Further, to analyze the magnetic nature of the compounds magnetic susceptibility is calculated by using the formula $\chi = \mu_B^2 N(E_F)$ and the results assured the AFM behavior of the compounds (Table 4).

The spin polarization (P) at the Fermi energy level is one of the important factors to resolve the superconducting point contact.^{30,31} The characterization of P is not significant when it is 0% and 100%. The intermediate spin polarizations have remarkable significance and it may support for superconductivity. The spin polarization at E_F (P) can be calculated as $P = N(E_F)\text{up} - N(E_F)\text{down}/N(E_F)\text{up} + N(E_F)\text{down}$ and the obtained values are presented in Table 4. The observed values are shown that, the bands of “s” and “d” orbital are the one of the factors to control P value. If the contribution from d -states increases, it leads to the increment in value of P . The total and partial Density of States histograms with spin (up and down) calculation for stable AFM state are shown in Figs. 1 and 2. The DoS histograms revealed that the major contribution of $N(E_F)$ is raised by Fe- d states than other elements/states and the same satisfies the above discussion about spin polarization (P) factor. Due to more hybridized $s - d$ bands in CaFe_2Bi_2 and SrFe_2As_2 compounds, the P value is less than other compounds.

BoltzTraP code interfaced in WIEN2K program is used to analyze the thermo electric properties of the projected compounds.³⁴ The computed electrical resistivity (ρ), Seebeck coefficient, electrical conductivity per unit relaxation time (σ/τ) and power factor are provided in Table 4 and the obtained values are agreed well with the existing results. The positive and negative Seebeck coefficient arises due to dominant hole and electron transport contribution, respectively.⁴⁰ The computed electrical resistivity value at 300 K of the parent and novel compounds is in the range of 0.01–1.28 $\mu\Omega\text{-cm}$ (Table 4) are feasible to predict the nature of superconductivity in these compounds. The same observation is supported from their conductivity

Table 4. Magnetic and thermoelectric transport properties and of (Ca/Sr/Ba)Fe₂(As/Bi)₂ in AFM (stabled) state.

Parameter	CaFe ₂ As ₂	CaFe ₂ Bi ₂	SrFe ₂ As ₂	SrFe ₂ Bi ₂	BaFe ₂ As ₂	BaFe ₂ Bi ₂
Total magnetic moment (μB)	2.7453	2.3400	2.5116	2.7055	2.4248	2.5110
Magnetic moment (μB) of Fe in compound	2.88 (up) (2.37) ³¹ 1.65 (dn) (Fe-1.6) ³² 43.36	2.71 (up) 1.63 (dn)	3.12 (up) 2.11 (dn) (Fe-1.8) ^{32,33}	2.86 (up) 1.74 (dn)	3.16 (up) 2.20 (dn) (Fe-1.8) ^{32,33}	2.85 (up) 1.83 (dn)
Spin polarization (P) in %		13.83	14.82	43.28	37.88	33.85
Susceptibility (χ) in 10^{-4} emu/mol	3.14 (3.7) ^{31,33}	3.53	3.5872	4.0870	3.033	2.481
Stoner criterion	1.75	1.87	2.0	2.28	1.68	1.38
Seebeck coefficient at 300 K (S) ($\mu\text{V}/\text{K}$)	-4.4320 (up) 5.1300 (dn) (5 ³⁵ , -5 ³⁶)	-15.0415 (up) 11.1017 (dn)	0.5778 (up) 0.3358 (dn)	17.1032 (up) 2.2088 (dn)	-1.2384 (up) -3.1040 (dn) (-2.5 ³⁷ , -5 ³⁸)	1.3371 (up) 0.0344 (dn)
Electrical resistivity (ρ) ($\mu\Omega\text{-cm}$) at 300 K	0.51 (up) 0.01 (dn)	1.28 (up) 0.6 (dn)	0.67 (up) 0.67 (dn)	0.66 (up) 0.58 (dn)	0.71 (up) (0.6 ³⁸) 1.25 (dn)	0.42 (up) 0.77 (dn)
Electrical conductivity/constant relaxation time at 300 K (σ/τ) 10^{21} ($\Omega^{-1} \text{m}^{-1} \text{s}^{-1}$)	0.1847(up) 0.0818(dn)	0.0780 (up) 0.1663 (dn)	0.1488 (up) 0.1488 (dn)	0.1527 (up) 0.1682 (dn)	17.72 (up) 10.03 (dn)	30.48 (up) 16.16 (dn)
Power factor [$\mu\text{W}/(\text{cm K}^2)$]	36.5 (up) 126 (dn)	158 (up) 164 (dn)	41.3 (up) 13.5 (dn)	357 (up) 0.02 (dn)	218 (up) 7.68 (dn)	4.28 (up) 38.3 (dn)
Electron phonon coupling constant (λ_{th})	0.3888	0.3838	0.3786	0.3842	0.3838	0.3841
Debye temperature θ_D (K)	281 (282) ⁴	186 (186) ⁴	280 (134,200) ⁴	118	111	283
Transition temperature T_c (K)	35 (≈ 25) ⁴⁶	21.27 (≈ 21) ⁴⁶	26.87 (≈ 22.5) ⁴⁶	12.87	12.05	30.78

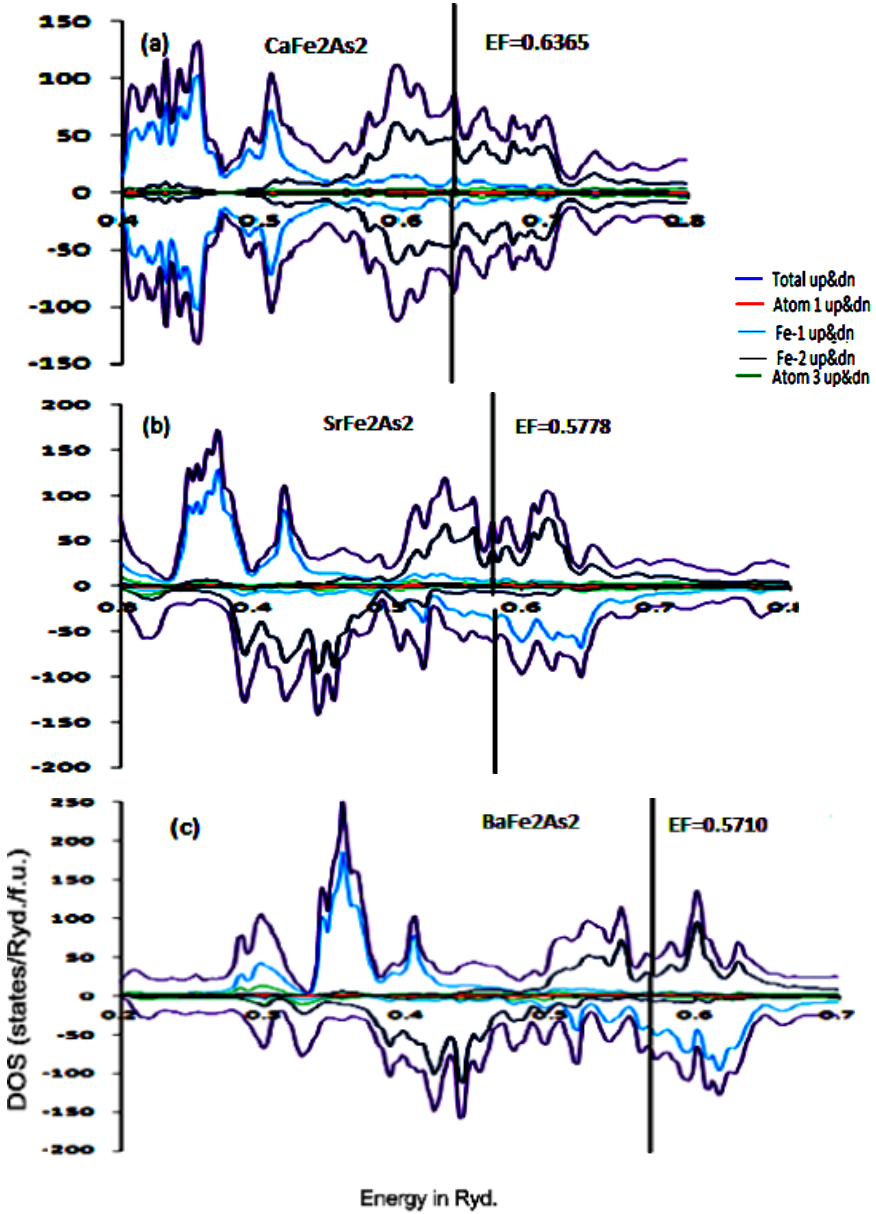


Fig. 1. (Color online) Total and partial spin-up and spin-down DOS histograms in AFM state (GGA+U) (a) CaFe₂As₂, (b) SrFe₂As₂ and (c) BaFe₂As₂.

values are in the range from $0.0780\tau \cdot 10^{21} \Omega^{-1} \text{ m}^{-1} \text{ s}^{-1}$ to $30.49\tau \cdot 10^{21} \Omega^{-1} \text{ m}^{-1} \text{ s}^{-1}$ and power factors upto $357 \mu\text{W}/(\text{cm K}^2)$.

The electron and phonon coupling factor should be less than 0.5 for unconventional superconductors.⁴¹ In order to improve the strength of our above discussions,

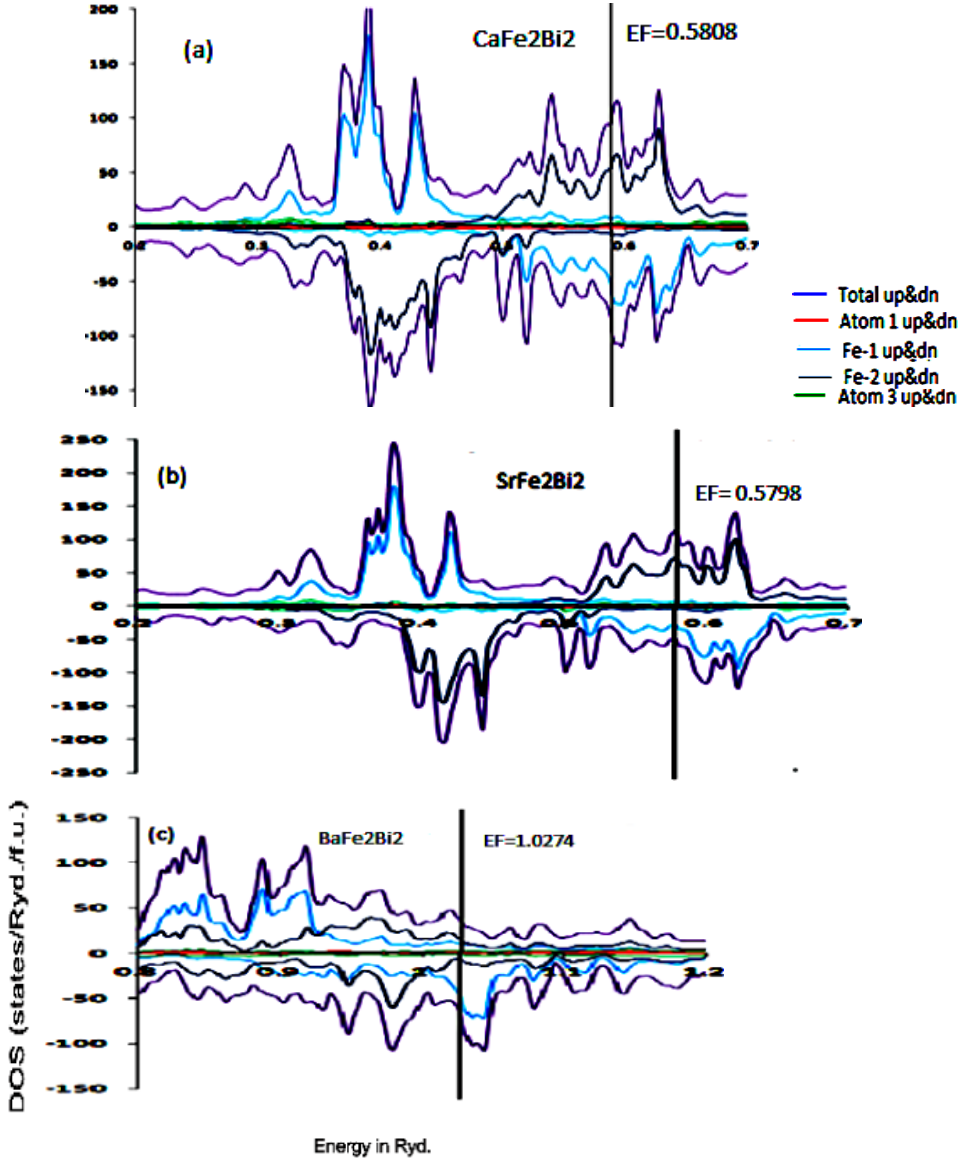


Fig. 2. (Color online) Total and partial spin-up and spin-down DOS histograms in AFM state (GGA+U) (a) CaFe_2Bi_2 , (b) SrFe_2Bi_2 and (c) BaFe_2Bi_2 .

the electron and phonon coupling constant is obtained by using the relation, $\lambda_{\text{th}} = 3\gamma/[2\pi^2 K_B^2 N(E_F)] - 1$ (see Ref. 42) and shown in Table 4. The obtained λ_{th} values (≈ 0.38) are not more than 0.5 and it helps to know about the possible superconducting nature of the proposed compounds. To extend our study, the superconducting transition/critical temperature is calculated for all the reported compounds. Hence, the Debye's temperature (θ_D) is calculated by using the relation,

$\theta_D = (h v_m / K_B) (6\pi^2 q / V)^{1/2}$ (see Ref. 43) where h is the Planck's constant, v_m is the elastic wave velocity, K_B is the Boltzmann's constant, q is the number of atoms in the unit cell and V is the volume of the unit cell. All these values are obtained by using tetra-elastic code.⁴⁴ By applying θ_D and λ_{th} values in McMillan Formula, the transition temperature (T_c) of the reported compounds is calculated as follows,⁴⁵ $T_c = \theta_D / 1.45 \exp [-(1.04(1+\lambda)/(\lambda - \mu^* - 0.62\lambda\mu^*))]$, where μ^* (0.13) is the Coulomb coupling constant and the calculated values of θ_D and T_c are presented in Table 4 and agreed well with available results. These values show that BaFe₂Bi₂ exhibits high T_c (30.78 K) than CaFe₂Bi₂ (12.97 K) and SrFe₂Bi₂ (12.05 K) compounds.

3.3. Mechanical properties and thermodynamic stability of the compounds

The tetra elastic code is used to compute the elastic parameters viz., c11, c33, c44, c66, c12 and c13 (Table 5). The observed results have good agreement with the available results. These elastic constants are used to check the Born mechanical stability criteria⁴⁹ and the conditions are $c_{11} > 0$, $c_{44} > 0$, $c_{66} > 0$, $c_{11} - c_{12} > 0$,

Table 5. Mechanical properties of (Ca/Sr/Ba)Fe₂(As/Bi)₂ in AFM (stabled) state.

Parameter	CaFe ₂ As ₂	CaFe ₂ Bi ₂	SrFe ₂ As ₂	SrFe ₂ Bi ₂	BaFe ₂ As ₂	BaFe ₂ Bi ₂
C ₁₁ (GPa)	103.08	157.6165	151.5507 (166) ⁴⁷	158.3187	116.12	286.2568
C ₁₂ (GPa)	37.0511	56.7841	27.7362 (30) ⁴⁷	43.7872	28.4828	276.4381
C ₁₃ (GPa)	57.6212	82.2714	31.7828 (36.8) ⁴⁷	62.6403	76.7827	117.4250
C ₃₃ (GPa)	138.8486	156.0884	82.0855 (65) ⁴⁷	86.2347	131.6611	13.3808
C ₄₄ (GPa)	78.1355	5.6176	3.8686 (0) ⁴⁷	4.8185	78.0881	127.1184
C ₆₆ (GPa)	114.5348	43.5272	70.1208 (80.5) ⁴⁷	10.6628	68.5273	11.5212
Bulk modulus (B) (GPa)	71.82 (70 ± 4) ⁴⁸	68	63	83	81 (67 ± 4) ⁴⁸	178
Shear modulus (G) (GPa)	31 (G_{min}) 115 (G_{max})	21	4 (G_{min}) 70 (G_{max})	12	18 (G_{min}) 78 (G_{max})	58
Young's modulus (E) (GPa)	77 (E_{min}) 186 (E_{max})	73	15 (E_{min}) 147 (E_{max})	36	53 (E_{min}) 174 (E_{max})	157
Poisson's ratio (σ) (GPa)	-0.42 (σ_{min}) 0.58 (σ_{max})	0.675	0.02 (σ_{min}) 0.88 (σ_{max})	0.426	-0.40 (σ_{min}) 0.80 (σ_{max})	0.35
Anisotropic factor (A^U)	8.3	6.5	3.1	1.2	2.6	2.8
Pugh ratio (G/B)	0.48	0.30	0.33	0.14	0.11	0.33

$2c_{11} + c_{33} + 2c_{12} + 4c_{13} > 0$, $c_{11} + c_{33} - 2c_{13} > 0.50$. These elastic constants are used to calculate Young's (E), bulk (B), shear (G) modulus and Poisson's ratio (σ). The universal anisotropy factor is given by, $A^U = 5G_V/G_R + B_V/B_R - 6$,⁴³ where G_V is Voigt shear modulus, G_R is Reuss Shear modulus, B_V is Voigt bulk modulus and B_R is Reuss bulk modulus, respectively. In an isotropic medium, A^U is zero and in anisotropic medium A^U is nonzero. The observed A^U values are presented in Table 5 and all these values are nonzero. Hence, the proposed materials are observed as highly anisotropic material. In our earlier work, an anisotropic nature of these materials is revealed from their electron density plots through bonding nature between the atoms.¹⁹ The existence of covalent bonding is in between Fe and As (Bi) atoms; metallic bonding exists in between As (Bi) and As (Bi) atoms and ionic bonding nature exists in between alkali earth metal (Ca/Sr/Ba) to FeAs(Bi) blocks. The mixed bonding nature reveals the anisotropic bonding nature of the proposed materials. The present study verified the same through its mechanical parameters. One of the evidences to find mechanical nature of the compound is Pugh's ratio (G/B); if G/B exceeds the value 0.5, the material is brittle and the lower value (<0.5) shows ductility nature. In this study, the compounds are exhibiting Pugh's ratio (Table 5) less than 0.5; hence, it indicates the ductile nature of the materials and the result is consistent with the earlier reports.⁵¹

Further, the elastic properties of all the materials are visualized by using Elate⁵² tool to analyze the elastic tensors. By using the elastic constants, the eigenvalues of the stiffness matrix ($\lambda_1, \lambda_2, \lambda_3, \lambda_4, \lambda_5, \lambda_6$ in GPa) are calculated. It helps to examine the mechanical stability and anomalous mechanical behavior of the compounds including the possibility for large negative linear compressibility or negative area compressibility or the potential for adsorption or pressure-induced large-scale structural transitions. Elate tool is used to obtain the 3D image of Young's modulus, Shear modulus and Poisson ratio by using the triangular form of 6×6 symmetric matrix of elastic constants and the obtained figures (Figs. 3–7) are used to analyze the distribution of elastic property along 3D axes. The different shape of the 3D images allows the determination of directions of particular interest in the

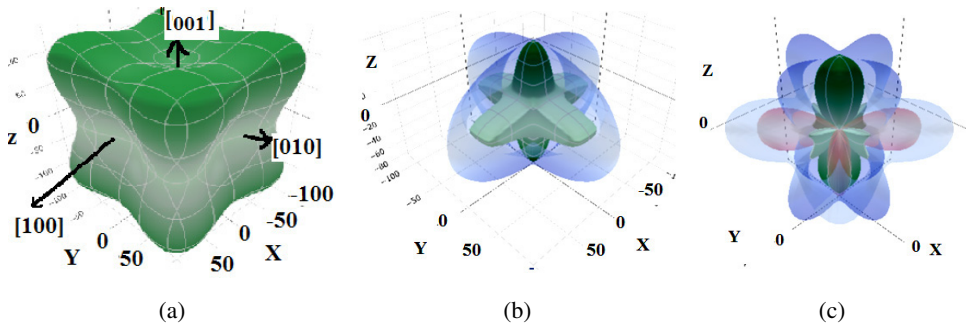


Fig. 3. (Color online) CaFe_2As_2 — (a) 3D Young modulus, (b) 3D Shear modulus and (c) 3D Poisson's ratio.

elastic properties, which are not necessarily along the crystallographic axes of the material. For a stable structure, the eigenvalues are positive and the stiffness matrix is invertible. The calculated eigenvalues of the stiffness matrix of CaFe_2As_2 (59,66,74,79,115,220); SrFe_2As_2 (4,4,65,70,124,197); BaFe_2As_2 (6,58,69,76,78,148); CaFe_2Bi_2 (1,3,6,6,44,167); SrFe_2Bi_2 (5,5,11,11,16,182) shows that the mechanical stability of these compounds. The eigenvalue of the stiffness matrix is negative for BaFe_2Bi_2 compound; it shows the mechanical instability of the system through the observation of elastic tensors and unable to plot 3D images of various moduli, but the same compound is satisfied under Born stability criteria. Hence, it may indicate the possibility of structural deformation of this compound due to external stress.⁵³ The plot of Young's modulus with their spherical coordinates at different directions is used to depict the features of elastic anisotropy; Directional dependence of Young's modulus figures of CaFe_2As_2 [Fig. 3(a)], BaFe_2As_2 [Fig. 5(a)], CaFe_2Bi_2 [Fig. 6(a)] shows that strong anisotropic properties in [100], [010] and [001] planes due to its lack of uniform distribution of stress and strain (Nonspherical curve). In

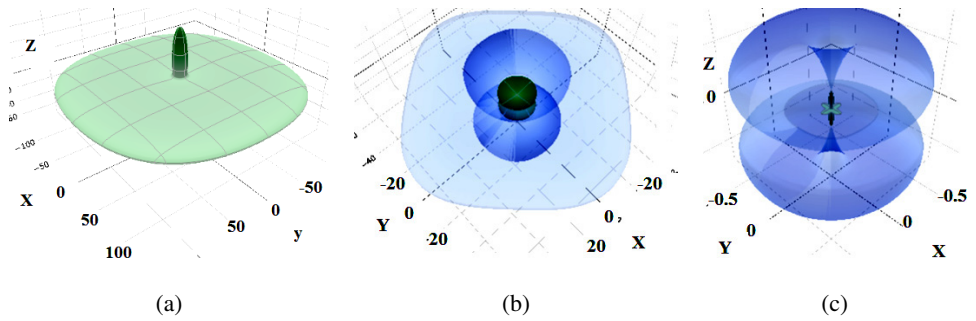


Fig. 4. (Color online) SrFe_2As_2 — (a) 3D Young modulus, (b) 3D Shear modulus and (c) 3D Poisson's ratio.

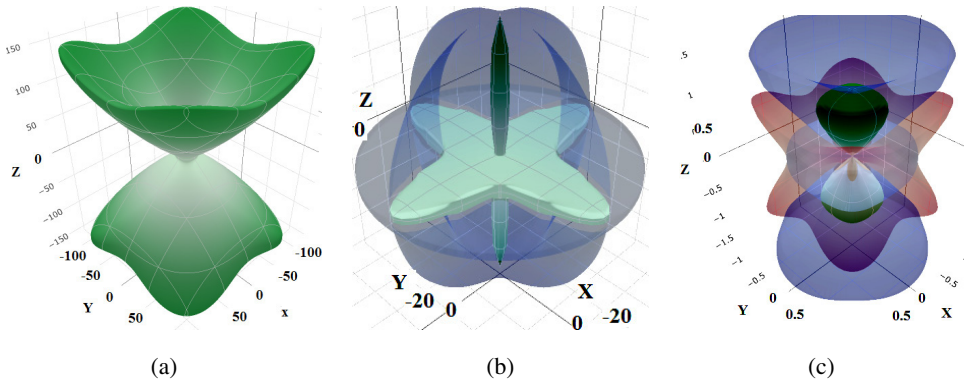


Fig. 5. (Color online) BaFe_2As_2 — (a) 3D Young modulus, (b) 3D Shear modulus and (c) 3D Poisson's ratio.

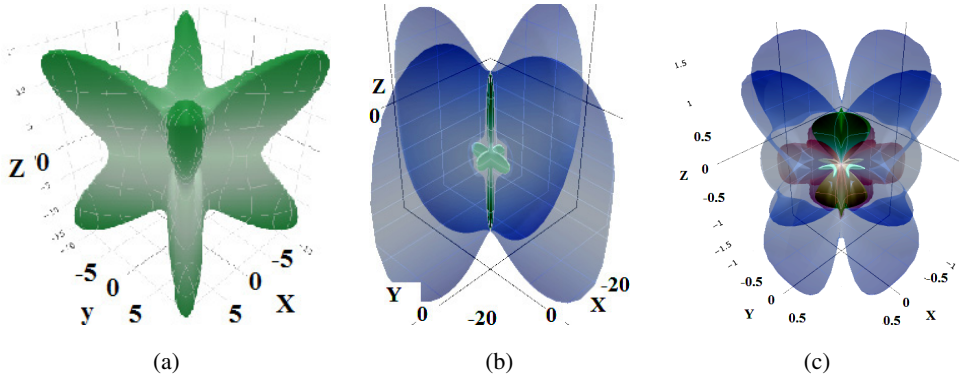


Fig. 6. (Color online) CaFe_2Bi_2 — (a) 3D Young modulus, (b) 3D Shear modulus and (c) 3D Poisson's ratio.

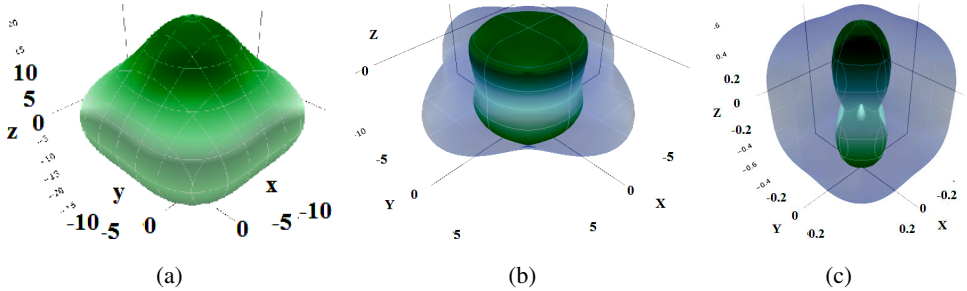


Fig. 7. (Color online) SrFe_2Bi_2 — (a) 3D Young modulus, (b) 3D Shear modulus and (c) 3D Poisson's ratio.

$\text{SrFe}_2(\text{As}/\text{Bi})_2$, [Figs. 4(a) and 7(a)] show that uniform distribution along x and y -axis but not along in z -axis [001], hence showing lower anisotropy than “Ca” and “Ba” based materials. The Shear modulus give the maximum (G_{\max}) along [001] direction while the G_{\min} along the [100] direction [Figs. 3(b), 4(b), 5(b), 6(b) and 7(b)] and the same reveals the anisotropic nature of the compound. The surface corresponding to the maximum Poisson ratio is shown in blue and the surface corresponding to the minimum Poisson ratio is shown in green [Figs. 3(c), 4(c), 5(c), 6(c) and 7(c)] along [001] plane. In these figures, the solid green lobes represent positive values of Poisson's ratio and translucent red lobes for negative values. From these observations, it shows that all the mechanical parameters are more dominant along [001] plane in the reported compounds.

The thermodynamic stability occurs when a system is in its lowest energy state or chemical equilibrium with its environment. Theoretically, the stability of a particular structure is derived by determining its minimum Gibbs free energy (G) using the relationship $G = E + PV + TS$, where E is the internal energy, P is the pressure, V is the volume and S is the vibrational entropy. These calculations have been performed for the reported compounds with the Gibbs2 code.⁵⁴ The

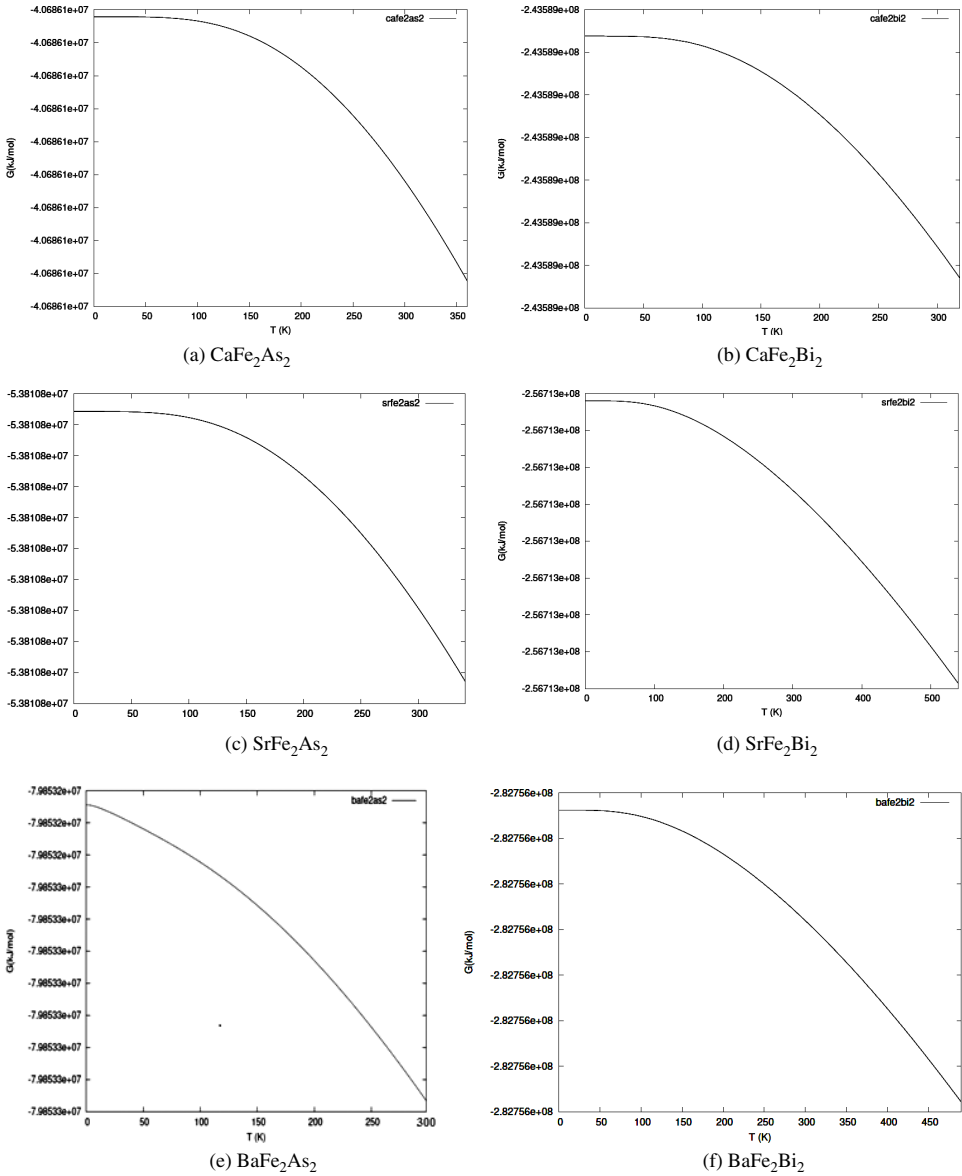


Fig. 8. Gibbs free energy versus temperature.

thermodynamic properties are determined by using quasi-harmonic Debye model which is implemented in Gibbs code and shown in Fig. 8. One can see that the Gibbs free energy, decreases slightly with increasing temperature in all the reported compounds and the same depicts the thermodynamic stability of the compounds. The trend followed in between the Gibbs free energy (G) and the temperature is same for parent compounds namely $(\text{Ca}/\text{Sr}/\text{Ba})\text{Fe}_2\text{As}_2$ shown in Figs. 8(a), 8(c) and 8(e)

and novel compounds namely (Ca/Sr/Ba)Fe₂Bi₂ are shown in Figs. 8(b), 8(d) and 8(f), respectively. The vibrational Helmholtz free energy is an important parameter to determine the dynamic stability of a structure. A structure with more negative value of the Helmholtz free energy will be considered to be more stable. In these reported compounds, Helmholtz free energy is found to be decreased on increasing temperature and the stability is confirmed.

4. Conclusion

The theoretically proposed CaFe₂Bi₂, SrFe₂Bi₂ and BaFe₂Bi₂ compounds are analyzed to understand their stable magnetic nature. By comparing the possible parameters such as total and formation energy, magnetic moment of these compounds in AFM, nonmagnetic (NM) and ferro magnetic (FM) orders, it is observed AFM is the stabled nature of the proposed materials. The comparative structural, electronic and magnetic properties analysis between (Ca,Sr,Ba)Fe₂Bi₂ and (Ca,Sr,Ba)Fe₂As₂ suggests that (Ca,Sr,Ba)Fe₂Bi₂ compounds are isostructural with experimentally reported superconducting (Ca,Sr,Ba)Fe₂As₂ compounds. The obtained resistivity 0.01–1.25 ($\mu\Omega$ -cm) of (Ca,Sr,Ba)Fe₂Bi₂ compounds provided a lead to the possible superconductivity nature of these compounds. These observations concluded that contemporaneous of superconductivity and AFM is possible in (Ca,Sr,Ba)Fe₂Bi₂ compounds alike their parent compounds. BaFe₂Bi₂ might exhibit high T_c (\approx 30 K) than other proposed materials. All the parent (Ca,Sr,Ba)Fe₂As₂ and novel (Ca,Sr,Ba)Fe₂Bi₂ materials exhibit ductile nature and are satisfied by Born stability criteria. (Ca,Ba)Fe₂(As/Bi)₂ materials exhibit strong anisotropic mechanical properties than SrFe₂(As/Bi)₂. Eigen values of the stiffness matrix gives a clue for possible phase transformation of BaFe₂Bi₂ compound.

Acknowledgments

The authors are acknowledged DST-FIST, India (Ref. No. SR/FSTPSI-183/2015).

References

1. F. Ma et al., *Front. Phys. China* **5**, 150 (2010).
2. I. R. Shein and A. L. Ivanovski, *Phys. Lett. A* **375**, 1028 (2011).
3. H. Hosono et al., *Mater. Today* **21**, 278 (2018).
4. F. Ronning et al., *J. Phys.: Condens. Matter* **20**, 322201 (2008).
5. F. Ronning et al., *Physica C* **468**, 386 (2008).
6. M. Rotter, M. Tegar and D. Johrendt, *Phys. Rev. Lett.* **101**, 107006 (2008).
7. Y. Tomioka et al., *Phys. Rev. B* **78**, 132506 (2008).
8. Y.-Z. Zhang et al., *Phys. Rev. B* **80**, 084530 (2008).
9. Y. Li and J. Ni, *Phys. Lett. A* **375**, 4218 (2011), doi:10.1016/j.physleta2011.10.011.
10. M. Sundareswari and M. Rajagopalan, *Int. J. Mod. Phys. B* **18**, 4587 (2005).
11. K. V. Guohe Huan Martha Greenblatt Ramanujachary, *Solid State Commun.* **71**, 221 (1888).
12. M. U. Salma and M. Atikur Rahman, *Int. J. Mod. Phys. B* **32**, 1850357 (2018).

13. I. H. A. Ouahab and A. Boukraa, *J. Supercond. Nov. Magn.* **30**, 2043 (2017).
14. C. M. Thompson *et al.*, *Solid State Commun.* **47**, 5563 (2011).
15. M. Pouchard, J.-P. Doumerc and A. Vilesuzanne, *Solid State Sci.* **12**, 681 (2010).
16. K. M. Gyu, Structural and magnetic properties of transition metal substituted BaFe₂As₂ compounds studied by X-ray and neutron scattering, Ph.D Thesis, 12852 (2012).
17. N. Kurita *et al.*, *J. Phys: Conf. Ser.* **273**, 012087 (2011).
18. A. Subedi and D. J. Singh, *Phys. Rev. B* **78**, 132511 (2008).
19. M. Sundareswari, D. S. Jayalakshmi and E. Viswanathan, *Philos. Mag.* **86**, 511 (2016).
20. K. Schwarz, P. Blaha and S. B. Trickey, *Mol. Phys.* **108**, 3147 (2010).
21. J. P. Perdew, K. Burke and M. Emzerhof, *Phys. Rev. Lett.* **77**, 3865 (1866).
22. F. Birch, *Phys. Rev.* **71**, 808 (1947).
23. H. L. Shi *et al.*, *J. Phys.: Condens. Matter* **22**, 125702 (2010).
24. D. S. Jayalakshmi and M. Sundareswari, *J. Alloys Compd.* **561**, 268 (2013).
25. J. Zhao *et al.*, *Nat. Phys.* **5**, 555 (2008).
26. B. Saparov and A. S. Sefat, *J. Solid State Chem.* **204**, 32 (2013).
27. I. R. Shein and A. L. Ivanovski, *Phys. Rev. B* 054510 (2008).
28. X. Tan, Z. P. Tener and M. Shatruk, *Acc. Chem. Res.* **51**, 230 (2018).
29. T. Beuerle *et al.*, *Phys. Rev. B* **48**, 8802 (1994).
30. R. J. Soulen *et al.*, *Science* **282**, 538685 (1998).
31. S. Ran *et al.*, *Phys. Rev. B* **83**, 144517 (2011).
32. K. Ali and K. Maiti, *Sci. Rep.*, arXiv:1703.07040v1.
33. D. Kasinathan *et al.*, *New J. Phys.* **11**, 025023 (2008).
34. G. K. H. Madsen and D. J. Singh, *Comput. Phys. Commun.* **175**, 67 (2006).
35. M. Matusiak, Z. Bukowski and J. Karpinski, *Phys. Rev. B* **81**, 020510 (2010).
36. G. Wu *et al.*, *J. Phys.: Condens. Matter* **20**, 422201 (2008).
37. S. Arsenijevic *et al.*, *Phys. Rev. B* **84**, 075148 (2011).
38. A. F. May *et al.*, *Phys. Rev. B* **88**, 064502 (2013).
39. A. Mani *et al.*, *Eur. Phys. Lett.* **87**, 17004 (2008).
40. I. P. F. Caglieris and M. Putti, *Supercond. Sci. Technol.* **28**, 073002 (2016).
41. L. Rettig *et al.*, *New J. Phys.* **15**, 083023 (2013).
42. Hadi *et al.*, *Chin. Phys. B* **26**, 037103 (2017).
43. S. Harish *et al.*, *Mod. Phys. Lett. B* **30**, 1650178 (2016).
44. A. H. Reshak and M. Jamal, *Int. J. Electrochem. Sci.* **8**, 12252 (2013).
45. D. S. Jayalakshmi and M. Sundareswari, *Ind. J. Phys.* **88**, 201 (2015).
46. D. Y. Chen *et al.*, *Chin. Phys. Lett.* **33**, 067402 (2016).
47. I. R. Shein and A. L. Ivanovski, *Physica C* **468**, 15 (2008).
48. M. T. R. Valent and H. O. Jeschke, *Phys. Rev. B* **85**, 084105 (2012).
49. M. Born, *J. Chem. Phys.* **7**, 581 (1939).
50. A. M. M. Tanveer Karim *et al.*, *J. Phys. Chem. Solids* **117**, 138 (2018).
51. N. Ni *et al.*, *Phys. Rev. B* **78**, 01452 (2008).
52. R. Gaillac, P. Pullumbi and F. Coudert, *J. Phys.: Condens. Matter* **28**, 275201 (2016).
53. J. L. Tallon and A. Wolfenden, *J. Phys. Chem. Solids* **40**, 831 (1979).
54. A. Otero-de-la-Roza, D. Abbasi-Pérez and V. Luaña, *Comput. Phys. Commun.* **182**, 2232 (2011).